

AD _____
(Leave blank)

Award Number: W81XWH-09-1-0232

TITLE: Materials to Engineer the Immune System

PRINCIPAL INVESTIGATOR: PI David J. Mooney

CONTRACTING ORGANIZATION: Harvard College President Fellows
Cambridge, MA 02138

REPORT DATE: April 2010

TYPE OF REPORT: Annual

PREPARED FOR: U.S. Army Medical Research and Materiel Command
Fort Detrick, Maryland 21702-5012

DISTRIBUTION STATEMENT:

X Approved for public release; distribution unlimited

The views, opinions and/or findings contained in this report are those of the author(s) and should not be construed as an official Department of the Army position, policy or decision unless so designated by other documentation.

REPORT DOCUMENTATION PAGE				Form Approved OMB No. 0704-0188	
Public reporting burden for this collection of information is estimated to average 1 hour per response, including the time for reviewing instructions, searching existing data sources, gathering and maintaining the data needed, and completing and reviewing this collection of information. Send comments regarding this burden estimate or any other aspect of this collection of information, including suggestions for reducing this burden to Department of Defense, Washington Headquarters Services, Directorate for Information Operations and Reports (0704-0188), 1215 Jefferson Davis Highway, Suite 1204, Arlington, VA 22202-4302. Respondents should be aware that notwithstanding any other provision of law, no person shall be subject to any penalty for failing to comply with a collection of information if it does not display a currently valid OMB control number. PLEASE DO NOT RETURN YOUR FORM TO THE ABOVE ADDRESS.					
1. REPORT DATE (DD-MM-YYYY) 30-04-2010		2. REPORT TYPE Annual		3. DATES COVERED (From - To) 1 April 2009 - 31 March 2010	
4. TITLE AND SUBTITLE Materials to Engineer the Immune System				5a. CONTRACT NUMBER W81XWH-09-1-0232	
				5b. GRANT NUMBER W91ZSQ8279N653	
				5c. PROGRAM ELEMENT NUMBER	
6. AUTHOR(S) Mooney, David J. Email: mooneyd@seas.harvard.edu				5d. PROJECT NUMBER	
				5e. TASK NUMBER	
				5f. WORK UNIT NUMBER	
7. PERFORMING ORGANIZATION NAME(S) AND ADDRESS(ES) President and Fellows of Harvard College 1350 Mass Ave Ste 600 Cambridge, MA 02138-3846				8. PERFORMING ORGANIZATION REPORT NUMBER	
9. SPONSORING / MONITORING AGENCY NAME(S) AND ADDRESS(ES) U.S. Army Medical Research and Materiel Command Fort Detrick, Maryland 21702-5012				10. SPONSOR/MONITOR'S ACRONYM(S)	
				11. SPONSOR/MONITOR'S REPORT NUMBER(S)	
12. DISTRIBUTION / AVAILABILITY STATEMENT Approved for public release; distribution unlimited.					
13. SUPPLEMENTARY NOTES					
14. ABSTRACT The ex vivo manipulation of cells central to current approaches to cancer vaccines imposes a large economic and regulatory burden, dendritic cell modifications may be dependent on culture conditions and transient, and the vast majority of transplanted cells die following transplantation, leading to weak immune responses. The long-term objective is to bypass ex vivo cell manipulation in breast cancer vaccines, and instead develop effective material systems that program the immune system in situ. The specific hypothesis being addressed in this project is that a material system providing appropriate spatiotemporal presentation of GM-CSF, CpG oligonucleotides and specific tumor antigens to host dendritic cells (DCs) can effectively recruit, program and disperse host dendritic cells, and the programmed dendritic cells will be capable of stimulating specific T-cell populations and eliciting a strong anti-tumor response. Studies to date strongly support this hypothesis, as we have shown that polymers presenting appropriate cytokines and immunostimulatory cues can recruit large numbers of dendritic cells and regulate their activation.					
15. SUBJECT TERMS Dendritic cells, GM-CSF, CpG, poly(lactide-co-glycolide)					
16. SECURITY CLASSIFICATION OF:			17. LIMITATION OF ABSTRACT UU	18. NUMBER OF PAGES 20	19a. NAME OF RESPONSIBLE PERSON USAMRMC
a. REPORT U	b. ABSTRACT U	c. THIS PAGE U			19b. TELEPHONE NUMBER (include area code)

Table of Contents

	<u>Page</u>
Introduction.....	1
Body.....	2-6
Key Research Accomplishments.....	6
Reportable Outcomes.....	6
Conclusion.....	6
References.....	6
Appendices.....	6

INTRODUCTION:

Cancer vaccines seek to prevent or treat breast cancer by activation of the immune system to destroy tumor cells. Ordinarily, the ability of tumor cells to stimulate an immune response is limited, in part, by weak expression of MHC-antigen complexes and costimulatory signals by antigen presenting cells that stimulate T-cell activation. Many experimental vaccines isolate and program dendritic cells (DCs) ex vivo by pulsing cultured cells with tumor associated antigens to bypass these issues, and introduce the programmed cells back into the patient where they may home to a lymph node, stimulate specific T-cell populations and elicit anti-tumor responses. While considerable progress has been made, the ex vivo manipulation of cells central to current approaches imposes a large economic and regulatory burden, DC modifications may be dependent on culture conditions and be transient, and the vast majority of transplanted cells die following transplantation, leading to weak immune responses. This application proposes a new approach to cancer vaccines, in which host cells are programmed in situ. We specifically propose to develop a material-based cancer vaccine that spatiotemporally controls the presentation of chemotactic factors and programming factors in situ in order to first recruit DCs, and secondly to program these cells with appropriate cues to elicit an effective antitumor response.

BODY:

Task 1: Developing system for GM-CSF tissue exposure to recruit dendritic cells

GM-CSF was embedded (54% efficiency) into poly(lactide-co-glycolide) (PLG) matrices using a high pressure, gas foaming process. Matrices were designed to release a pulse of GM-CSF to recruit DCs, and were loaded with 0, 3000, and 7000 ng of GM-CSF and implanted into the subcutaneous pockets of C57BL/6J mice. A GM-CSF gradient formed in the surrounding tissue, with concentrations peaking at 12 hours post-implantation as the GM-CSF concentration reached 100 µg/ml and 30 µg/ml (>30 fold difference over no incorporated GM-CSF) at distances of 1-3mm and 3-5mm, respectively, from the implant site (Fig. 1). Elevated GM-CSF levels were maintained for extended periods (approximately 10 days). Histological analysis at day 14 post-implantation of PLG matrices loaded with 3000 ng of GM-CSF revealed enhanced cellular infiltration over blank controls (Fig. 2A), and FACS analysis for the CD11c(+) DC population showed that GM-CSF delivery recruited significantly more DCs (~8 fold increase) than blank PLG matrices (Fig. 2B). The matrix-resident DCs were almost exclusively CD11b+ (~87%), in accordance with other reports of GM-CSF effects on DC development in vivo. The total number of DCs recruited and their expression of the co-stimulatory molecule CD86 increased with GM-CSF delivery in a dose dependent manner (Fig. 2D). However, the highest dose (7000 ng) of GM-CSF reduced the number of activated DCs at the implant site, as indicated by diminished MHCII and CCR7 expression at day 14 post implantation (Fig 2D & Fig. 3). Since total DC recruitment and activation both peaked with the 3000ng dose, this dose was utilized to recruit and generate DCs in subsequent studies. Importantly, GM-CSF promoted greater cellular penetration into and association with the PLG material, potentially allowing for the subsequent programming of resident DC precursors and DCs.

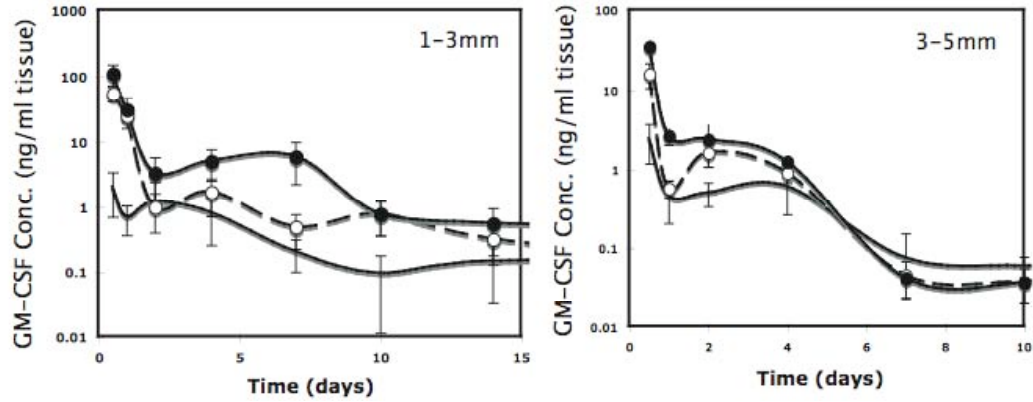


Fig. 1. The in vivo concentration profiles of GM-CSF in adjacent tissue at distances of 1-3 mm and 3-5 mm away from the implant site of PLG matrices as a function of time post implantation into subcutaneous pockets of C57BL/6J mice. Matrices contained initial dosages of 0 (—), 3000 (---○---), and 7000 ng (---●---) of GM-CSF.

Task 2: Utilizing local CpG presentation to control maturation and lymph node homing of dendritic cells

The local presentation of danger signals to regulate the ratio of distinct DC subtypes was next examined, by modifying PLG matrices to immobilize TLR-activating, PEI-condensed CpG-ODN molecules, and present them to cell populations recruited by GM-CSF. Stimulation with CpG-ODN alone enriched the PLG matrix with CD11c(+)PDCA-1(+) pDCs (Fig. 4A), and this was increased with co-administration of GM-CSF (Fig. 4B). The dose of CpG-ODN presented in combination with 3000ng GM-CSF was altered to regulate the numbers of resident plasmacytoid dendritic cells (pDCs), which increased from 190,000, to 520,000, and to 1,200,000 cells at doses of 0, 10 and 100 μ g of CpG-ODN, respectively (Fig. 4B). Co-presentation of CpG-ODN had little effect on the ability of GM-CSF to enhance CD11c+CD11b+ cDCs (Fig. 4C). High doses of CpG-ODN promoted the local production of IFN- α (~1010 pg/ml) and IFN- γ (~600 pg/ml), independently of the presence of GM-CSF (Fig. 4E & 4F). These results indicate that controlled GM-CSF and CpG-ODN danger signaling from synthetic extra-cellular matrices cooperate to regulate resident pDC and CD11c(+)CD11b(+) cDC numbers, along with the production of protective cytokines commonly linked to Th1 and cytotoxic T lymphocyte immunity.

Task 3: Immunologic response to neu antigen and over-expressing tumors

No progress to date.

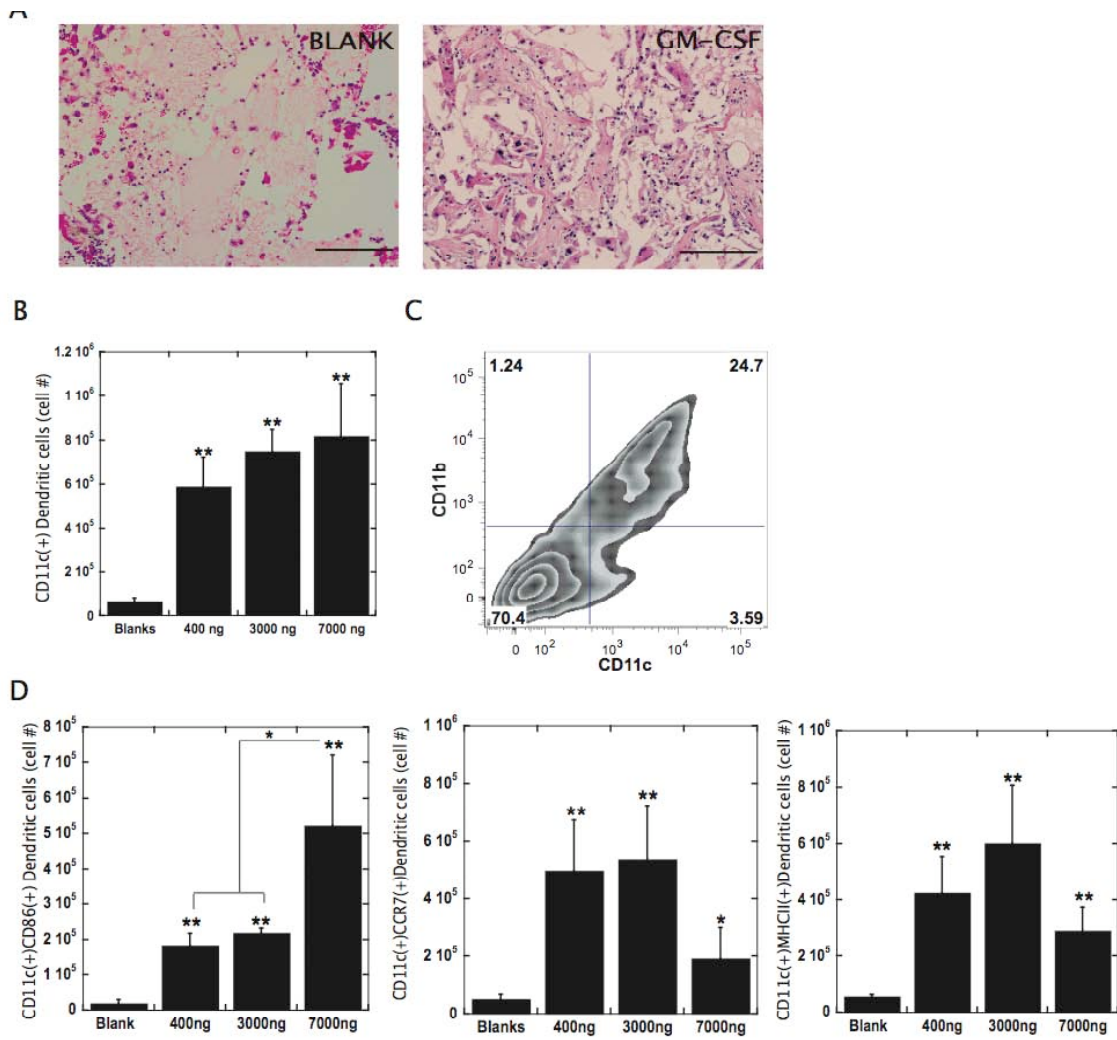


Fig. 2 GM-CSF delivery from PLG matrices promotes CD11b+ DC recruitment and activation. (A) H&E staining of sectioned PLG scaffolds explanted from subcutaneous pockets in the backs of C57BL/6J mice after 14 days: Blank scaffolds (BLANK), and GM-CSF (3000 ng) loaded scaffolds (GM-CSF). (B) The number of CD11c(+) DCs isolated from PLG scaffolds at day 14 after implantation in response to doses of 0, 1000, 3000 and 7000 ng of GM-CSF. (C) FACS plots of cells isolated from explanted scaffolds and stained for CD11c and CD11b. Cells were isolated from PLG matrices incorporating 3,000ng of GM-CSF at day 10 post-implantation. Numbers in FACS plots indicate the percentage of the cell population positive for CD11c and CD11b or for both markers. (D) The number of CD11c(+)CD86(+), CD11c(+)CCR7(+), and CD11c(+)MHCII(+) DCs isolated from PLG scaffolds at day 14 after implantation in response to doses of 0, 400, 3000 and 7000 ng of GM-CSF. Values in B and D represent mean and standard deviation (n=4 or 5). * $P < 0.05$ ** $P < 0.01$ as compared to blank matrices unless otherwise noted.

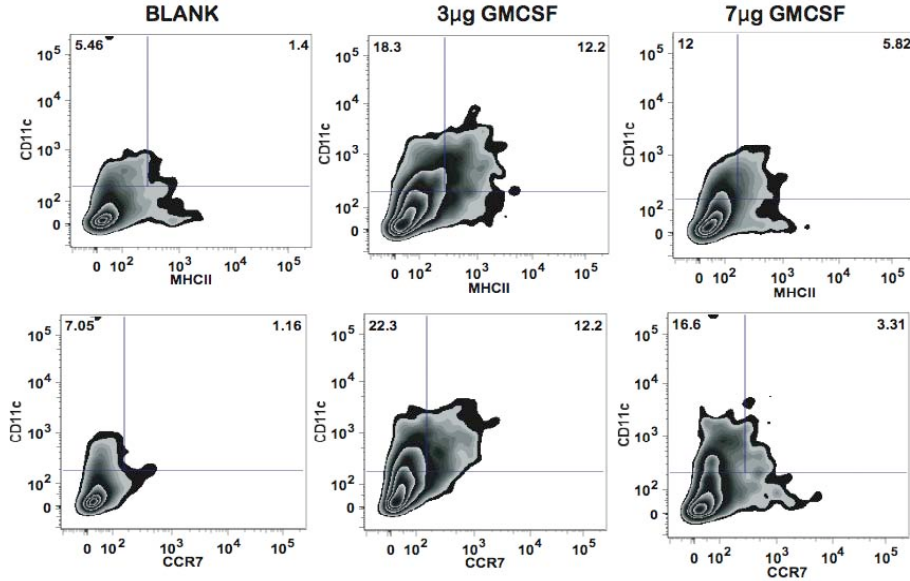


Fig. 3. FACS plots of cells isolated from explanted scaffolds and stained for the DC marker, CD11c and for activation markers MHCII and CCR7. Cells were isolated from Blank PLG matrices or matrices incorporating either 3 or 7 µg of GM-CSF at day 14 post-implantation. Numbers in FACS plots indicate the percentage of the cell population positive for CD11c only or positive for both CD11c and either MHCII or CCR7.

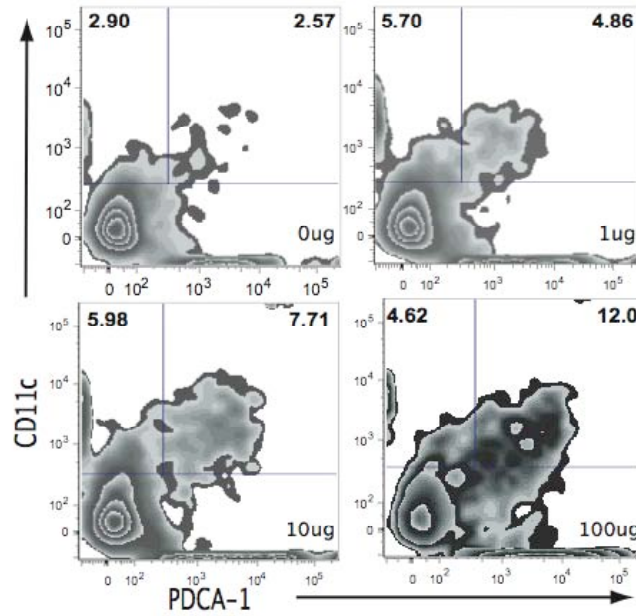
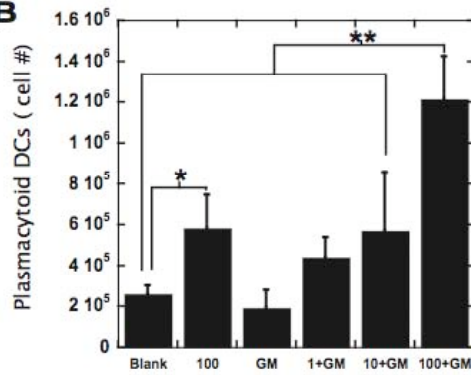
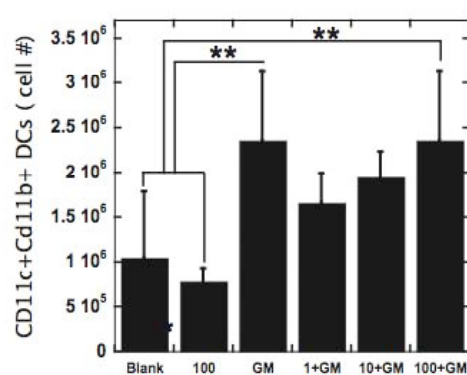
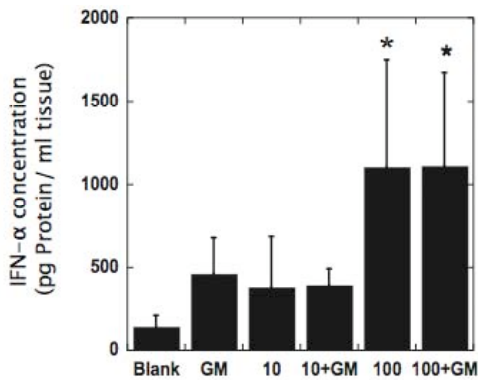
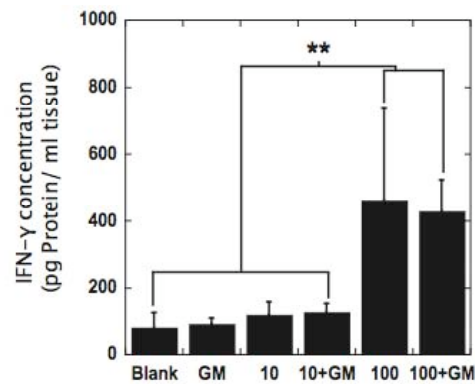
A**B****C****D****E**

Figure 4. CpG-ODN and GM-CSF delivery from PLG matrices promotes plasmacytoid DC generation and the production of anti-tumor cytokines. (A) FACS plots of cells isolated from explanted scaffolds and stained for the plasmacytoid DC markers, CD11c and PDCA-1. Cells were isolated from PLG matrices incorporating 0, 1, 10, and 100 µg of CpG-ODN at day 10 post-implantation. Numbers in FACS plots

indicate the percentage of the cell population positive for CD11c only or for both markers. The number of (B) plasmacytoid DCs, and (C) CD11c(+)CD11b(+) cDCs at day 10 post-implantation in blank scaffolds (Blank) or in response to doses of 100 µg (100) of CpG-ODN or 3000ng GM-CSF alone (GM) or GM-CSF in combination with 1 (1+GM), 10 (10+GM), or 100 µg (100+GM) of CpG-ODN. The in vivo concentrations of (D) IFN- α , and (E) IFN- γ at Day 10 post implantation at the implant site of blank PLG matrices (Blank), or matrices loaded with 3000ng GM-CSF alone (GM) or 10µg or 100µg (100) of CpG-ODN alone or GM-CSF in combination with 10 (10+GM), or 100 µg (100+GM) of CpG-ODN. Values in B-E represent mean and standard deviation (n=4 or 5). * $P < 0.05$ ** $P < 0.01$ as compared to blank matrices unless otherwise noted.

KEY RESEARCH ACCOMPLISHMENTS:

- Demonstrated sustained and localized release of GM-CSF from polymers can recruit large numbers of dendritic cells.
- Local presentation of CpG in concert with GM-CSF allows one to control the types and numbers of dendritic cells at the vaccine site.

REPORTABLE OUTCOMES:

- Ali O, Emerich D, Dranoff G, Mooney DJ. In situ regulation of DC subsets and T cells mediates tumor regression in mice. **Sci Transl Med.** 2009 Nov; 1(8): 8ra19
- Omar Ali hired by InCytu Inc (start-up company) based on the research experience he obtained while working on this project

CONCLUSION:

The results to date indicate that material systems can recruit and activate large numbers of dendritic cells, and generate the types of dendritic cells and microenvironment consistent with generation of a destructive immune response. This suggests one may be able to bypass ex vivo cell manipulation, and directly program dendritic cells already existing in the body to generate an immune response to cancer. These are exciting findings, and support the premise underlying this project.

REFERENCES:

None

APPENDICES:

Attached published article:

Ali OA, Emerich D, Dranoff G, Mooney DJ. In Situ Regulation of DC Subsets and T Cells Mediates Tumor Regression in Mice. *Sci Transl Med.* 2009 Nov; 1(8): 8ra19.

SUPPORTING DATA:

None

A complete electronic version of this article and other services, including high-resolution figures, can be found at:

<http://stm.sciencemag.org/content/1/8/8ra19.full.html>

Supporting Online Material can be found at:

"[Supplementary Material](#)"

<http://stm.sciencemag.org/content/suppl/2009/11/21/1.8.8ra19.DC1.html>

This article **cites 42 articles**, 15 of which can be accessed free:

<http://stm.sciencemag.org/content/1/8/8ra19.full.html#ref-list-1>

Information about obtaining **reprints** of this article or about obtaining **permission to reproduce this article** in whole or in part can be found at:

<http://www.sciencemag.org/about/permissions.dtl>

In Situ Regulation of DC Subsets and T Cells Mediates Tumor Regression in Mice

Omar A. Ali,^{1,2,3} Dwaine Emerich,² Glenn Dranoff,^{4,5} David J. Mooney^{1,3*}

(Published 25 November 2009; Volume 1 Issue 8 8ra19)

Vaccines are largely ineffective for patients with established cancer, as advanced disease requires potent and sustained activation of CD8⁺ cytotoxic T lymphocytes (CTLs) to kill tumor cells and clear the disease. Recent studies have found that subsets of dendritic cells (DCs) specialize in antigen cross-presentation and in the production of cytokines, which regulate both CTLs and T regulatory (Treg) cells that shut down effector T cell responses. Here, we addressed the hypothesis that coordinated regulation of a DC network, and plasmacytoid DCs (pDCs) and CD8⁺ DCs in particular, could enhance host immunity in mice. We used functionalized biomaterials incorporating various combinations of an inflammatory cytokine, immune danger signal, and tumor lysates to control the activation and localization of host DC populations in situ. The numbers of pDCs and CD8⁺ DCs, and the endogenous production of interleukin-12, all correlated strongly with the magnitude of protective antitumor immunity and the generation of potent CD8⁺ CTLs. Vaccination by this method maintained local and systemic CTL responses for extended periods while inhibiting FoxP3 Treg activity during antigen clearance, resulting in complete regression of distant and established melanoma tumors. The efficacy of this vaccine as a monotherapy against large invasive tumors may be a result of the local activity of pDCs and CD8⁺ DCs induced by persistent danger and antigen signaling at the vaccine site. These results indicate that a critical pattern of DC subsets correlates with the evolution of therapeutic antitumor responses and provide a template for future vaccine design.

INTRODUCTION

Dendritic cells (DCs) are promising effectors of immunotherapy as they are essential for initiating and regulating T cell immunity. The interaction between DCs and pathogens can lead to antigen capture and processing by DCs. Pathogen-associated molecular patterns, including lipopolysaccharides and cytosine-guanosine (CpG)-rich sequences in pathogenic DNA, activate DCs via ligation of particular Toll-like receptors (TLRs), which stimulate DC expression of specific costimulatory molecules and cytokines capable of propagating the appropriate T cell response. Activated DCs migrate to lymphoid tissues where they present pathogenic antigens and stimulatory molecules to naïve T cells, leading to T cell activation, expansion, and specific responses.

Chronic exposure to tumor antigens with inappropriate costimulation and immunomodulation by T regulatory (Treg) cells allows solid tumors to develop by dysregulating DC activity and the cytotoxic T lymphocyte (CTL) responses required to kill tumor cells (1, 2). Cancer vaccines are frequently developed with easily accessible, patient-derived blood monocytes that are transformed into DCs ex vivo with cytokine mixtures and pulsed with tumor antigens to promote antigen presentation (3–5). These antigen-loaded DCs are then infused back into cancer patients with the goal of inducing antitumor immune responses mediated primarily by T helper 1 (T_H1) cells and CTLs (3–5). Although clinical trials using such ex vivo DC vaccines in patients with advanced cancer have resulted in antigen-specific T cell expansion

and the production of protective cytokines in vivo (2–6), many vaccines do not increase patients' survival over traditional treatments (for example, chemotherapy) (2) and have failed to consistently cause the regression of solid tumors (1–4). In both murine models and humans, these strategies are likely unable to generate the necessary numbers of functional CD8⁺ CTLs for the duration required to induce regression of solid invasive tumors in both mice and humans. Instead, they may amplify defective CTLs that never become fully functional effectors at the tumor site because of high local concentrations of immunosuppressive cytokines [for example, transforming growth factor-β (TGF-β) and interleukin-10 (IL-10)] and Treg cells, which dampen immune responses (1, 2).

Hematopoietic precursor cells of both the myeloid and lymphoid lineage have the capacity to differentiate into two main categories of DCs: conventional DCs (cDCs) and plasmacytoid DCs (pDCs) (7–9). Effective cancer vaccines may require both types of DCs, as each is equipped with a specific defense mechanism in response to invading pathogens. cDCs include CD11c⁺CD11b⁺ and CD11c⁺CD8⁺ cells and exhibit classic DC morphology, protruding dendrites that make these cells especially adept at antigen processing and antigen presentation to T cells (7–9). Plasmacytoid DCs exhibit a spherical morphology (7) and can produce large amounts of type 1 interferons (IFNs) in response to “danger signals,” such as unmethylated CpG dinucleotide sequences found in bacterial or viral DNA (7, 10, 11). Plasmacytoid DC-derived type 1 IFNs link innate and adaptive immunity to viral infection by directly inducing naïve T cell differentiation to T_H1 cells (10–12) and by triggering antigen cross-presentation to CD8⁺ T cells (13, 14) and IL production (for example, IL-12) by cDCs that facilitate the clonal expansion of CTLs. The plasticity of hematopoietic precursors likely allows for the recruitment and generation of the DC population most proficient at eliciting the appropriate immune response in a particular situation (7–9, 13). Current vaccines are unable to recapitulate

¹School of Engineering and Applied Sciences, 29 Oxford Street, 319 Pierce Hall, Harvard University, Cambridge, MA 02138, USA. ²InCytu Inc., 701 George Washington Highway, Lincoln, RI 02865, USA. ³Wyss Institute for Biologically Inspired Engineering, Cambridge, MA 02138, USA. ⁴Department of Medical Oncology and Cancer Vaccine Center, Dana-Farber Cancer Institute, Boston, MA 02115, USA. ⁵Department of Medicine, Brigham and Women's Hospital and Harvard Medical School, Boston, MA 02115, USA.

*To whom correspondence should be addressed. E-mail: mooneyd@seas.harvard.edu

ex vivo the development of this broad DC response, which is critical to the development of potent CTL immune responses (3, 4).

Here, we have hypothesized that one can manipulate the in situ generation of a heterogeneous DC network capable of CTL induction, and activate robust CD8⁺ T cell effector responses to established tumors, by providing a secondary immunostimulatory site of tumor antigen presentation. Inflammation or infection can produce DC populations

that are not found in the steady state (15), which suggests that stimuli in tissue microenvironments provoke a response from the network of DCs. The cytokine granulocyte-macrophage colony-stimulating factor (GM-CSF) is present at increased concentrations during inflammation (16, 17), which may cause the recruitment of both monocytes and DCs while inducing local monocytes to differentiate into DCs (15, 17–19). Recently, we described the development of implantable synthetic polymer matrices that spatially and temporally control the in vivo presentation of cytokines, tumor antigens, and danger signals (20). GM-CSF is released from these polylactide-co-glycolide (PLG) [a Food and Drug Administration (FDA)-approved biomaterial] matrices into the surrounding tissue to recruit DC precursors and DCs. CpG-rich oligonucleotides are immobilized on the matrices as danger signals, and antigen (tumor lysates) is released to matrix-resident DCs to program DC development and maturation. These matrices quantitatively regulate DC activation and trafficking in situ and induce prophylactic immunity against inoculations of murine B16-F10 melanoma cells (14). Here, we have investigated the ability of this system to control the recruitment and activation of multiple DC and T cell subsets and to provide therapeutic vaccination against established tumors.

RESULTS

Local GM-CSF delivery promotes recruitment of CD11b⁺ DCs

As described previously (20), macroporous PLG matrices were fabricated for GM-CSF release to recruit DCs and with an interconnected porous structure that allows for cell infiltration (10). Matrices were loaded with 0, 3000, and 7000 ng of GM-CSF and implanted into the subcutaneous pockets of C57BL/6J mice. Histological analysis at day 14 after implantation of PLG matrices loaded with 3000 ng of GM-CSF revealed enhanced cellular infiltration when compared to blank controls (Fig. 1A). Fluorescence-activated cell sorting (FACS) analysis for CD11c⁺ DCs showed that GM-CSF delivery recruited significantly more DCs (a factor of ~8 increase) than blank PLG matrices (Fig. 1B). The matrix-resident DCs were almost exclusively CD11b⁺ (~87%) (Fig. 1C), in accordance with other studies of GM-CSF effects on DC recruitment in vivo (21, 22). The total number of DCs recruited and their expression of the costimulatory molecule CD86 increased with GM-CSF delivery in a dose-dependent manner (Fig. 1D). However, the highest dose (7000 ng) of GM-CSF reduced the number of activated DCs at the implant site, as indicated by diminished major histocompatibility complex class II (MHCII) and CCR7 expression at day 14 after implantation (Fig. 1, E and F, and fig. S1). Because total DC recruitment and activation both peaked at 3000 ng of GM-CSF, this dose was used to recruit and generate DCs in subsequent studies. GM-CSF delivery promoted greater cellular penetration into and association with the PLG material, as indicated by histological analysis (Fig. 1A) and measurement of DC numbers (Fig. 1, B and D), potentially allowing for the subsequent programming of resident DC precursors and DCs.

In situ delivery of CpG-oligodeoxynucleotide promotes pDC recruitment and IFN production

The ability of local presentation of danger signals to regulate the ratio of distinct DC subtypes was next examined by immobilizing TLR-activating, polyethylenimine (PEI)-condensed CpG-oligodeoxynucleotide (ODN) molecules into the matrices. As described previously for plasmid DNA (20), condensation of oligonucleotides with the polycationic polymer

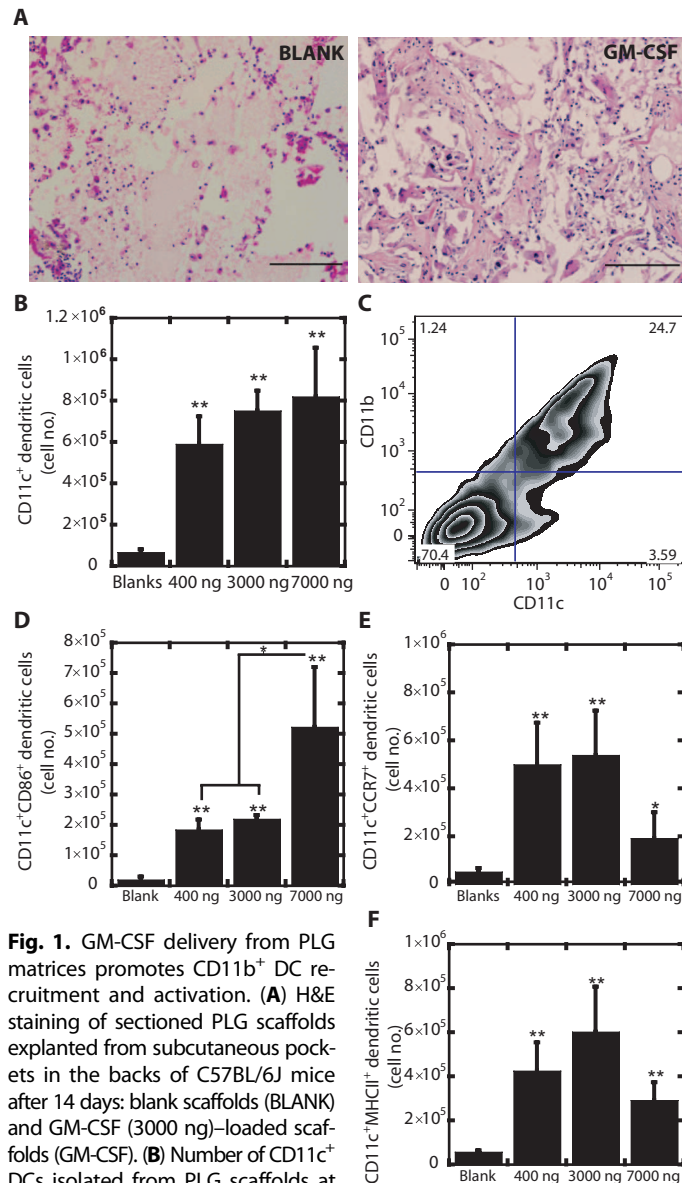


Fig. 1. GM-CSF delivery from PLG matrices promotes CD11b⁺ DC recruitment and activation. **(A)** H&E staining of sectioned PLG scaffolds explanted from subcutaneous pockets in the backs of C57BL/6J mice after 14 days: blank scaffolds (BLANK) and GM-CSF (3000 ng)-loaded scaffolds (GM-CSF). **(B)** Number of CD11c⁺ DCs isolated from PLG scaffolds at day 14 after implantation in response to doses of 0, 1000, 3000, and 7000 ng of GM-CSF. **(C)** FACS plots of cells isolated from explanted scaffolds and stained for CD11c and CD11b. Cells were isolated from PLG matrices incorporating 3000 ng of GM-CSF at day 10 after implantation. Numbers in FACS plots indicate the percentage of the cell population positive for CD11c and CD11b or for both markers. **(D to F)** Number of CD11c⁺CD86⁺ (D), CD11c⁺CCR7⁺ (E), and CD11c⁺MHCII⁺ (F) DCs isolated from PLG scaffolds at day 14 after implantation in response to doses of 0, 400, 3000, and 7000 ng of GM-CSF. Scale bar in (A), 100 μm. Values in (B) and (D) to (F) represent mean and SD (*n* = 4 or 5). **P* < 0.05, ***P* < 0.01 versus blank matrices unless otherwise noted.

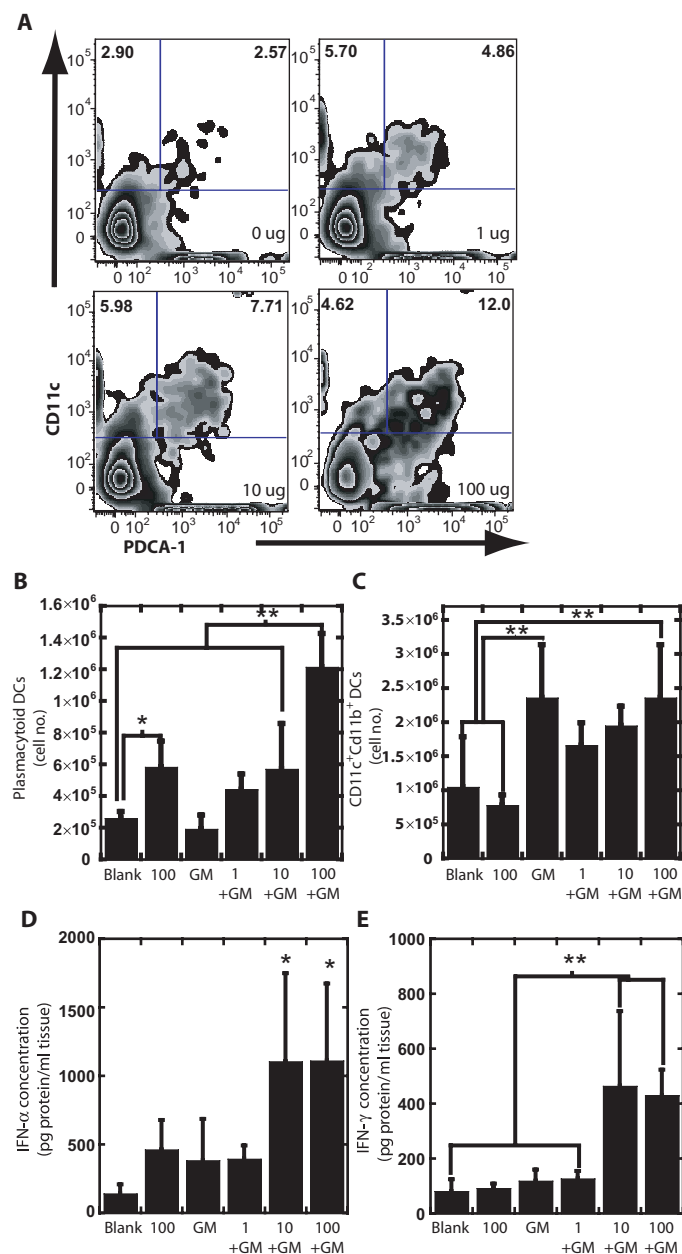


Fig. 2. CpG-ODN and GM-CSF delivery from PLG matrices promotes pDC generation and the production of antitumor cytokines. **(A)** FACS plots of cells isolated from explanted scaffolds and stained for the pDC markers CD11c and PDCA-1. Cells were isolated from PLG matrices incorporating 0, 1, 10, and 100 µg of CpG-ODN at day 10 after implantation. Numbers in FACS plots indicate the percentage of the cell population positive for CD11c only or for both markers. **(B and C)** The number of pDCs **(B)** and CD11c⁺CD11b⁺ cDCs **(C)** at day 10 after implantation in blank scaffolds (Blank) or in response to doses of 100 µg (100) of CpG-ODN or 3000 ng of GM-CSF alone (GM) or GM-CSF in combination with 1 µg (1+GM), 10 µg (10+GM), or 100 µg (100+GM) of CpG-ODN. **(D and E)** The in vivo concentrations of IFN-α **(D)** and IFN-γ **(E)** at day 10 after implantation at the implant site of blank PLG matrices (Blank) or matrices loaded with 3000 ng of GM-CSF alone (GM) or 10 µg or 100 µg (100) of CpG-ODN alone or GM-CSF in combination with 10 µg (10+GM) or 100 µg (100+GM) of CpG-ODN. Values in **(B)** to **(E)** represent mean and SD ($n = 4$ or 5). * $P < 0.05$, ** $P < 0.01$ as compared to blank matrices unless otherwise noted.

PEI results in positively charged particles that bind electrostatically to the anionic PLG matrix. PLG matrices incorporating CpG-ODN alone recruited CD11c⁺PDCA-1⁺ pDCs to the PLG matrix (Fig. 2A), and this effect was enhanced with coadministration of GM-CSF (Fig. 2B). We altered the dose of CpG-ODN presented in combination with 3000 ng of GM-CSF to regulate the numbers of resident pDCs, resulting in 190,000, 520,000, and 1,200,000 cells at doses of 0, 10, and 100 µg of CpG-ODN, respectively (Fig. 2B). Copresentation of CpG-ODN had little effect on the ability of GM-CSF to enhance CD11c⁺CD11b⁺ cDCs (Fig. 2C). High doses of CpG-ODN promoted the local production of IFN-α (~1010 pg/ml) and IFN-γ (~600 pg/ml) particularly in the presence of GM-CSF (Fig. 2, D and E). These results indicate that controlled GM-CSF and CpG-ODN danger signaling from synthetic extracellular matrices cooperates to regulate resident pDC and CD11c⁺CD11b⁺ cDC numbers, along with the production of protective cytokines commonly linked to T_H1 and CTL immunity.

Tumor lysate co-delivery with CpG-ODN and GM-CSF stimulates CD8⁺ DC generation and IL-12 production

We then hypothesized that copresenting cancer antigens with CpG-ODNs to matrix-resident DCs would promote further DC development, activation, and CTL antigen sensitization. In this context, necrotic tumor cells may be particularly immunostimulatory, as they release a variety of endogenous mediators (for example, heat shock proteins and damaged nucleic acids) that trigger innate immune recognition (23). Thus, freeze-thaw lysates of B16 melanomas were prepared, and antigen-presenting matrices were fabricated by encapsulating these lysates into the PLG material, resulting in localized and sustained antigen presentation to the infiltrating cell population (20). These antigen-presenting matrices unexpectedly stimulated CD8⁺ DC generation in situ (Fig. 3A). On viral invasion, CD8⁺CD11c⁺ cDCs are especially efficient at cross-presenting exogenous antigen on MHCI molecules (13, 14, 24–26) and at producing the T_H1-promoting cytokine IL-12 (13, 27–30), which are two mechanisms that aid in priming CTL immunity to viruses and tumors. This activity, however, is normally associated with lymphoid tissues (7, 9, 14, 24–26). Copresentation of tumor lysates with CpG-ODN led to the presence of 200,000 CD8⁺ DCs, which increased to ~670,000 (a factor of 9 increase over blank matrices) when GM-CSF was added to stimulate recruitment (Fig. 3B). Additionally, tumor lysate in combination with GM-CSF and CpG enhanced the numbers of recruited pDCs at day 10 after implantation by a factor of 2 over matrices without lysate and by a factor of 10 over blank controls (Fig. 3C). No significant difference in pDC numbers was observed with tumor lysate in combination with only GM-CSF or CpG signaling. The CD11c⁺CD11b⁺ DC population at the vaccine site depended mainly on GM-CSF (Fig. 3D), as tumor lysate or CpG signaling alone or in combination had no significant effect on the recruitment and expansion of these DCs (Fig. 3D).

It is interesting that the in situ production of the T cell growth factor IL-12 at matrices that deliver both tumor lysate and CpG-ODN to cell populations recruited by GM-CSF was about four times that of blank matrices and at least twice that of all other matrix formulations (Fig. 3E). However, tumor lysates in the matrix did not increase the high concentrations of IFN-α and IFN-γ induced by CpG-ODN and GM-CSF (Fig. 3, F and G). These results suggest that the engineered matrices manipulated both the number and the function of specific DC subsets, as well as the accompanying CTL-polarizing activity.

PLG matrices co-delivering GM-CSF, CpG-ODN, and tumor lysates stimulate potent local and systemic CD8⁺ cytotoxic T cells

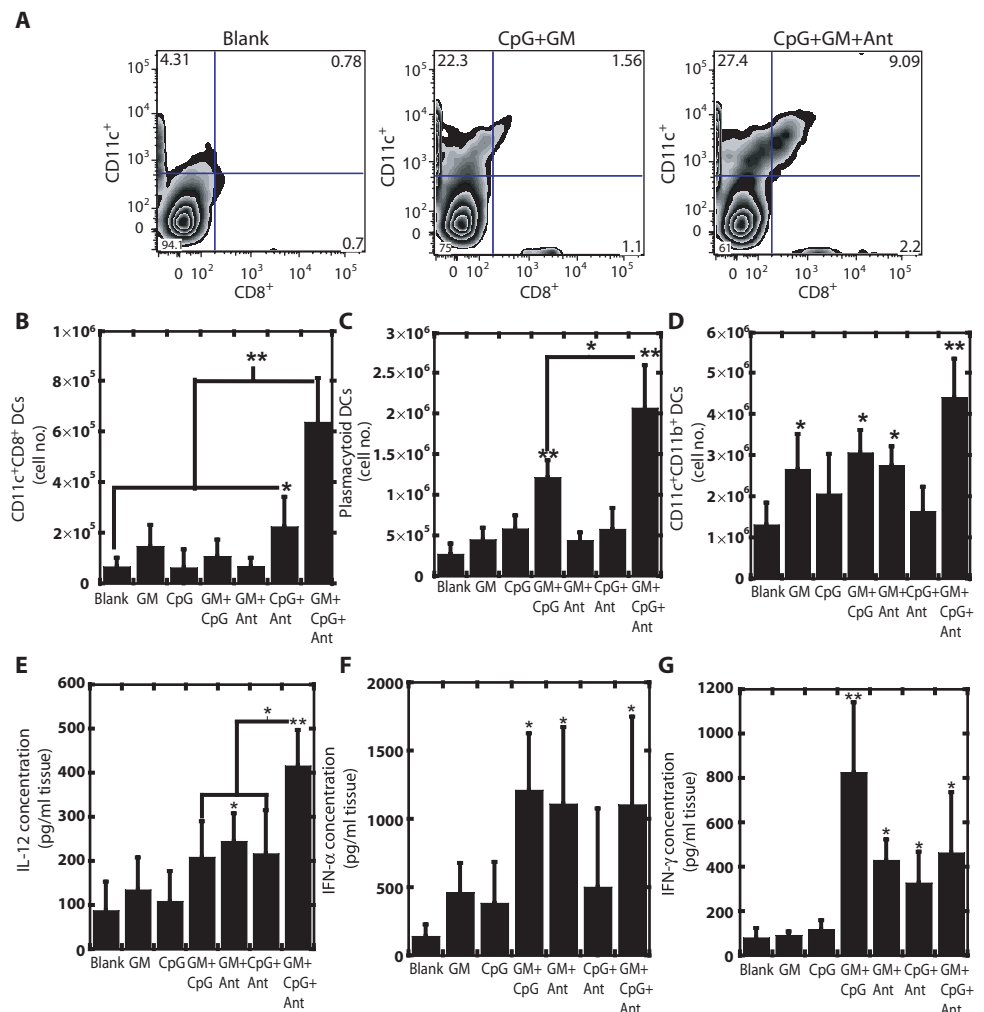
To elucidate the adaptive immune mechanisms induced by PLG vaccines that deliver tumor lysate, GM-CSF, and CpG-ODN, we examined the activity of both local and systemic CTLs. Flow cytometric analysis of cells infiltrating the vaccine site revealed a significant CD3⁺CD8⁺ T cell response by day 5 (representative sample: $\sim 1.9 \times 10^5$ cells), which peaked at day 12 when a relatively large proportion of the matrix-resident cells were CTLs (representative sample: 8.5% of cells; $\sim 8.5 \times 10^5$ cells) (Fig. 4A). Local CD8⁺ T cell numbers dropped sharply by day 16 and were negligible at day 21 (Fig. 4B) likely because of antigen clearance. PLG vaccines containing tumor lysates, GM-CSF, and CpG-ODN preferentially tuned and promoted CD8⁺ cytotoxic immune responses relative to other matrix formulations devoid of CpG (Fig. 4C). Further, the activation and persistence of systemic CTL responses was monitored by staining splenocytes with MHCI-tyrosinase-related protein 2 (TRP2) peptide pentamers to identify CTLs with specificity to TRP2, which is a major antigenic target of melanoma vaccines in mice and humans. A significant expansion of TRP2-specific CTLs was observed in the spleens of vaccinated mice by day 5, which continued and peaked between days 7 and 16 before falling at days 21 to 28 (Fig. 4, D and E),

indicating that systemic antimelanoma responses were being generated and sustained for extended periods.

Tumor protection induced by PLG matrices correlates with DC subsets and IL-12 production

It was previously demonstrated that this system is capable of generating prophylactic immunity against poorly immunogenic B16-F10 melanoma (20). The relation of this antitumor efficacy to the specific DC networks invoked by various vaccine formulations was investigated. C57BL/6J mice were vaccinated with PLG-based matrices incorporating B16 tumor lysates, GM-CSF, and CpG-ODN in varying combinations and then challenged with live B16-F10 melanoma tumor cells at day 14 after vaccination. PLG vaccines with both B16-F10 tumor lysates and 1, 10, 50, or 100 μ g of CpG-ODN danger signaling allowed 10 to 30% of the vaccinated mice to survive, tumor-free (Fig. 5A), after an otherwise lethal cell challenge, whereas 100% of unvaccinated mice were killed by day 23 due to tumor burden. When GM-CSF-mediated DC recruitment was combined with lysate and CpG-ODN delivery, the mice showed significant protection from tumor-induced lethality. CpG-ODN doses of 10, 50, and 100 μ g resulted in 50%, 60%, and 90% survival rates, respectively (Fig. 5B).

Fig. 3. Tumor lysate, CpG-ODN, and GM-CSF co-delivery from PLG matrices stimulates CD8⁺ DC generation and IL-12 production. **(A)** FACS density plots of CD11c and CD8 staining of cells infiltrating blank PLG matrices (Blank) or matrices loaded with 3000 ng of GM-CSF and 100 μ g of CpG-ODN without (CpG+GM) or with tumor lysates (CpG+GM+Ant) at day 10. Numbers in FACS plots indicate the percentage of the cell population positive for CD11c (upper left quadrant of each plot) and CD8 (lower right) or for both markers (upper right). **(B to D)** Number of CD11c⁺CD8⁺ cDCs (B), pDCs (C), and CD11c⁺CD11b⁺ cDCs (D) at day 10 after implantation in blank matrices (Blank) and in response to 3000 ng of GM-CSF (GM) or 100 μ g of CpG-ODN (CpG) alone or in combination (CpG+GM) or copresented with tumor lysates (GM+Ant, CpG+Ant, and CpG+GM+Ant). **(E to G)** In vivo concentration of IL-12 (E), IFN- α (F), and IFN- γ (G) at day 10 after implantation in blank matrices (Blank) and in response to doses of 3000 ng of GM-CSF (GM) or 100 μ g of CpG-ODN (CpG) alone or in combination (CpG+GM) or copresented with tumor lysates (GM+Ant, CpG+Ant, and CpG+GM+Ant). Values in (B) to (G) represent mean and SD ($n = 4$ or 5). * $P < 0.05$, ** $P < 0.01$ versus blank matrices, unless otherwise noted.



The ability of vaccine systems to create a heterogeneous DC population correlated with the marked increase in antitumor efficacy. In comparison to antigen matrices delivering GM-CSF alone, the antigen-loaded matrices delivering CpG and GM-CSF together resulted in a higher proportion of pDCs (~31% versus 7%) and CD8⁺ cDCs (~14% versus 5.5%) (Fig. 5C), which correlated with a significant enhancement in mouse survival (90% versus 20%), although total DC numbers in situ were statistically similar (3.0 ± 0.6 versus 4.2 ± 0.9 million DCs; two-tailed Student's *t* test, *n* = 5). Survival rates were proportional to the number of pDCs and CD8⁺ cDCs, but not CD11b⁺ DCs, generated at the PLG vaccine site at day 10 (Fig. 5, D to F). Additionally, the endogenous production of IL-12 was correlated with animal survival (Fig. 5G), suggesting the importance of cross-presentation and T_H1-promoting cytokines to vaccine efficacy.

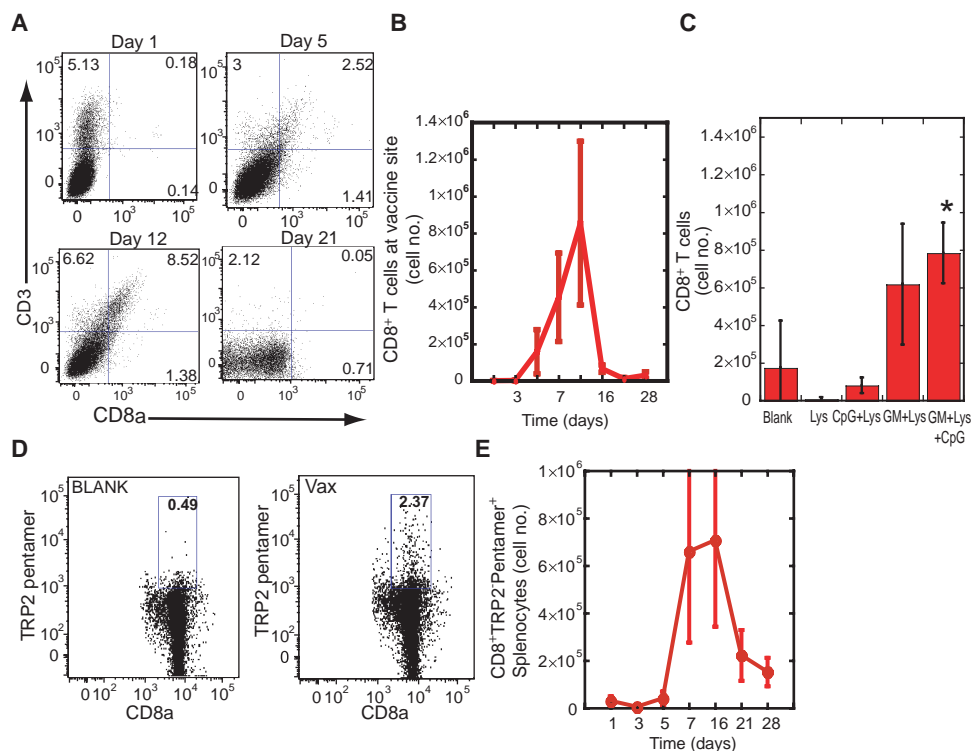
Engineered PLG matrices incorporating CpG-ODN attenuate immune regulation by FoxP3⁺ Treg number and immunosuppressive cytokines

Although several vaccines designed to program DCs either ex vivo or in situ have achieved significant and long-term prophylactic protection in mouse models of cancer (1, 4, 15), eradication of invasive and well-established tumors has not been achieved without adoptive T cell transfer or systemic therapies (1, 2, 31, 32). This limitation might reflect, at least in part, the ability of DC-based vaccines to stimulate Treg cells (33, 34) that attenuate the cytotoxic activity of adaptive immune responses. Thus, we characterized the

impact of the engineered matrices on the induction of immunosuppressive pathways. Monitoring CD4⁺ T cell responses to antigen-presenting matrices with GM-CSF and CpG revealed peak activity at days 5 and 7, which decreased to negligible concentrations by day 12 after implantation (Fig. 6A). In contrast, matrices containing GM-CSF and tumor lysate led to a significant enhancement of CD4⁺ T cell infiltration at day 12 (Fig. 6B), and these cells likely contribute to regulation of CTL responses. Incorporation of GM-CSF and tumor lysate into the vaccine matrix led to a factor of 10 increase in TGF- β concentrations (Fig. 6C) and a significant increase in IL-10 (Fig. 6D) at the vaccine site; these are cytokines commonly associated with Treg activity and immunosuppression. Further, as observed previously in GM-CSF-based vaccines (33, 34), GM-CSF cosignaling with tumor antigens resulted in a significant CD3⁺FoxP3⁺ response at the vaccine site (Fig. 6, E and F) when compared to all other matrix formulations, resulting in an almost even ratio of CD8⁺ effectors and FoxP3 Treg cells (Fig. 6G). CpG-ODN presentation in concert with both tumor lysate and GM-CSF counteracted these immunosuppressive mechanisms, as TGF- β and IL-10 concentrations and Treg activity were not enhanced over the control matrices, and CD8⁺ CTLs outnumbered FoxP3⁺ T cells by a factor of ~25 at day 12 after implantation (Fig. 6, C to G). Altogether, these findings suggest that this vaccine system is able to promote and extend CTL responses likely through naïve T cell differentiation induced by pDCs and CD8⁺ DCs, the corresponding production of type 1 IFNs and IL-12, and inhibition of negative feedback mechanisms.

Fig. 4. Tumor lysate, CpG-ODN, and GM-CSF co-delivery in PLG matrices stimulates

potent local and systemic CD8⁺ cytotoxic T cells. **(A)** FACS plots of cells isolated from explanted matrices and stained for the cytotoxic T cell markers CD3 and CD8a. Cells were isolated from PLG matrices with 3000 ng of GM-CSF, 100 μ g of CpG-ODN, and tumor lysates at days 1, 5, 12, and 21 after implantation. Numbers in FACS plots indicate the percentage of the cell population that was either single positive for CD3 (upper left quadrant of each plot) or CD8 (lower right) or double positive for both markers (upper right). **(B)** Total number of CD3⁺CD8⁺ cytotoxic T cells isolated from PLG matrices loaded with GM-CSF, CpG-ODN, and tumor lysates as a function of time after implantation. **(C)** Number of CD8 T cells at day 12 after implantation in blank scaffolds (Blank) or in response to lysate alone (Lys) or in combination with CpG-ODN (CpG+Lys) or GM-CSF (GM+Lys) or both factors (GM+Lys+CpG). **(D)** FACS plots of splenocytes of mice implanted with blank PLG matrices mice vaccinated with PLG vaccines containing 3000 ng of GM-CSF, 100 μ g of CpG-ODN, and tumor lysates at day 16 after implantation. Cells were stained with PE-conjugated antibody to CD8 and Kb-TRP2 pentamers. The gates represent the TRP2-specific CD8⁺ T cells, and numbers provide the percentage of gated cells. **(E)** Total number of TRP2-specific CD8⁺ T cells in the spleens of mice vaccinated with PLG



matrices loaded with GM-CSF, CpG-ODN, and tumor lysates as a function of time after implantation. Values in (B), (C), and (E) represent mean and SD (*n* = 4 or 5). **P* < 0.05 versus all other experimental conditions.

Engineered PLG matrices cause regression of established melanoma

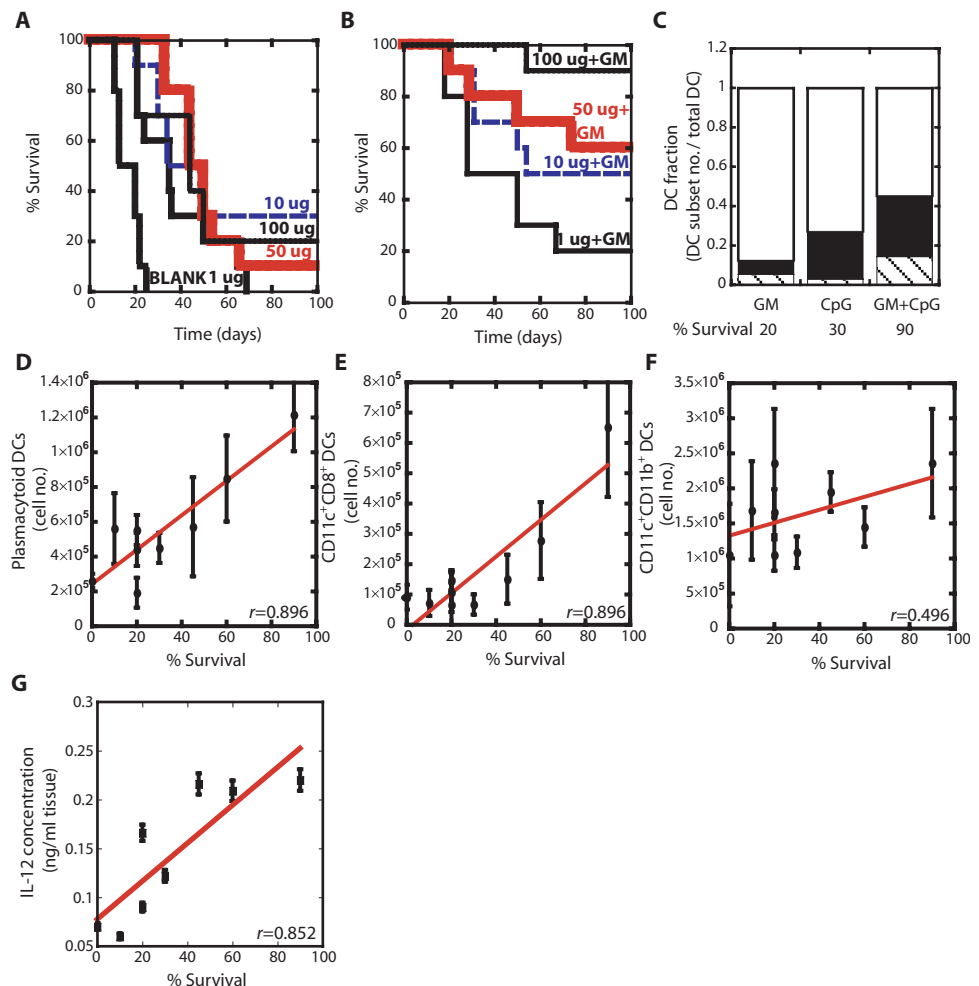
Because a high ratio of CD8⁺ T cell effectors to FoxP3⁺ Treg cells has been linked to therapeutic tumor immunity in murine and human systems (33, 35), we tested the activity of PLG vaccines against B16-F10 tumors that had been established for 9 days (inoculation of 5×10^5 cells at day 0). Tumor-bearing mice implanted with blank PLG matrices displayed rapid tumor growth and were killed by day 24, as expected (Fig. 7A). Vaccination of mice once with the PLG vaccine significantly decreased the rate of tumor progression (Fig. 7A), and an increase in mean survival time over controls was observed, but all animals required euthanization by day 58, depending on the tumor size at the time of vaccination (Fig. 7B). Vaccination of mice twice (days 9 and 19) with PLG vaccines had a more dramatic effect on tumor progression and caused complete regression of tumors in a subset (7 of 15) of the animals (Fig. 7C). In contrast, a single treatment with irradiated, GM-CSF-secreting B16-F10 cells, a widely used cell therapy now in clinical trials, attenuated tumor progression modestly, and all animals had to be killed by day 36 (Fig. 7A). Tumor antigen presentation from PLG matrices enhanced protection and was required to induce tumor regression,

as matrices with GM-CSF and CpG did not enhance survival times significantly (Fig. 7, A and B). Strikingly, 47% of the mice (animals bearing day 9 tumors) vaccinated twice with PLG vaccines survived long-term and free of detectable tumors; this treatment regimen was able to completely eradicate tumors of up to 25 mm² in size (Fig. 7C).

To test whether PLG vaccines could be effective against an even greater tumor burden, we established melanoma tumors for 13 days and then vaccinated the mice. One-time (day 13) and two-time (days 13 and 23) vaccination decreased tumor progression (Fig. 7D). Two-time vaccination doubled the mean survival time and led to complete tumor regression in 20% of the animals with advanced solid tumors (day 13 tumors; $n = 15$) (Fig. 7, D to F).

Because vaccinations were initiated at days 9 and 13 of tumor growth, and required 5 days for CTL generation, the effector window for immune responses was small (about 6 to 10 days) before untreated animals succumbed to tumor burden. Variations in tumor size at the time of vaccination likely accounted for the lack of complete regression in all animals; vaccination may not have resulted in generation of sufficient numbers of killer T cell in time to control and clear larger tumors. Slight hair loss and depigmentation was observed at the vac-

Fig. 5. Tumor protection stimulated by engineered PLG matrices is correlated with DC subsets and IL-12 production. Survival times of mice vaccinated with PLG vaccines 14 days before B16-F10 melanoma tumor challenge (10^5 cells). (A) Comparison of survival times in mice treated with blank PLG matrices or with PLG matrices loaded with tumor lysates and 1, 10, 50, or 100 μ g of CpG-ODN. (B) Comparison of survival times in mice vaccinated with PLG matrices loaded with tumor lysates, 3000 ng of GM-CSF, and 1, 10, 50, or 100 μ g of CpG-ODN. (C) Fraction of the total CD11c⁺ DC population consisting of CD11b⁺ cDCs (white bar), PDCA-1⁺ pDCs (black bar), and CD8⁺ cDCs (striped bar) generated at the PLG vaccine site at day 10. Vaccines were loaded with either 3000 ng of GM-CSF or 100 μ g of CpG-ODN alone or in combination. Survival percentages recorded at day 100 after tumor challenge. (D to G) Plots of the numbers of CD11c⁺PDCA-1⁺ pDCs (D), CD11c⁺CD8⁺ cDCs (E), and CD11c⁺CD11b⁺ cDCs (F) and the concentration of IL-12 at the PLG vaccine site (G) at day 10 versus the percent of animals surviving B16-F10 melanoma tumor challenge at day 100 [survival data taken from experimental conditions in (A) and (B)]. Values in (D) to (G) represent mean and SD ($n = 4$ or 5). r values in (D) to (F) represent the linear correlation coefficient between DC numbers or IL-12 concentration and survival percentage.



cine site, in agreement with the past study using this vaccination system (20), but no significant toxicities were observed with vaccination.

DISCUSSION

Current approaches to cancer vaccination augment cellular and humoral antitumor reactions in many patients, but most immunized subjects still succumb to progressive disease, indicating that vaccine responses are insufficient to effect complete tumor cell killing (1–4, 36). Nonetheless, the abilities of blocking antibodies to CTL-associated antigen-4 and the adoptive transfer of T cells in lymphodepleted hosts to accomplish tumor regressions highlight the potential for immune-mediated destruction of advanced cancer (35, 37). In this study, we demonstrate that the appropriate regulation of the DC network can induce complete regressions of distant and established melanomas in mice.

Our engineered PLG vaccine evokes a coordinated response of multiple DC subtypes, which together trigger sustained and potent antitumor CD8⁺ CTLs while inhibiting immunoregulatory pathways.

The combination of tumor cell lysates, GM-CSF, and CpG-ODN in the vaccine matrix was required for optimal tumor protection, which was strongly associated with the recruitment of pDCs and CD8⁺ DCs and the local production of IL-12. The accumulation of CD8⁺ DCs at the vaccine site is a notable feature of this vaccination strategy because this DC subset is typically localized to secondary lymphoid structures. Plasmacytoid DC numbers were closely linked with the generation of type I IFNs, as described in previous studies (10, 21, 38), and these cells helped to support the activation of CD8⁺ DCs and their cross-presentation of tumor antigens to T_H1 cells and CTLs (7–9, 13, 27). Further studies will elucidate which of the correlative observations in this study underlie the superior antitumor effect, as well as the mechanisms by which the vaccine may modulate other components of the immune system [for example, myeloid-derived suppressor cells that suppress GM-CSF-based vaccines (39)]. However, many cancer vaccination strategies use GM-CSF-stimulated monocyte-derived cDCs (3–5) as immunogens, and our experiments indicate that the presence of a broader set of DC subtypes may evoke more potent antitumor responses.

Our findings also suggest that a minimum number of DCs may be required to induce high concentrations of protective immunity. Vaccines

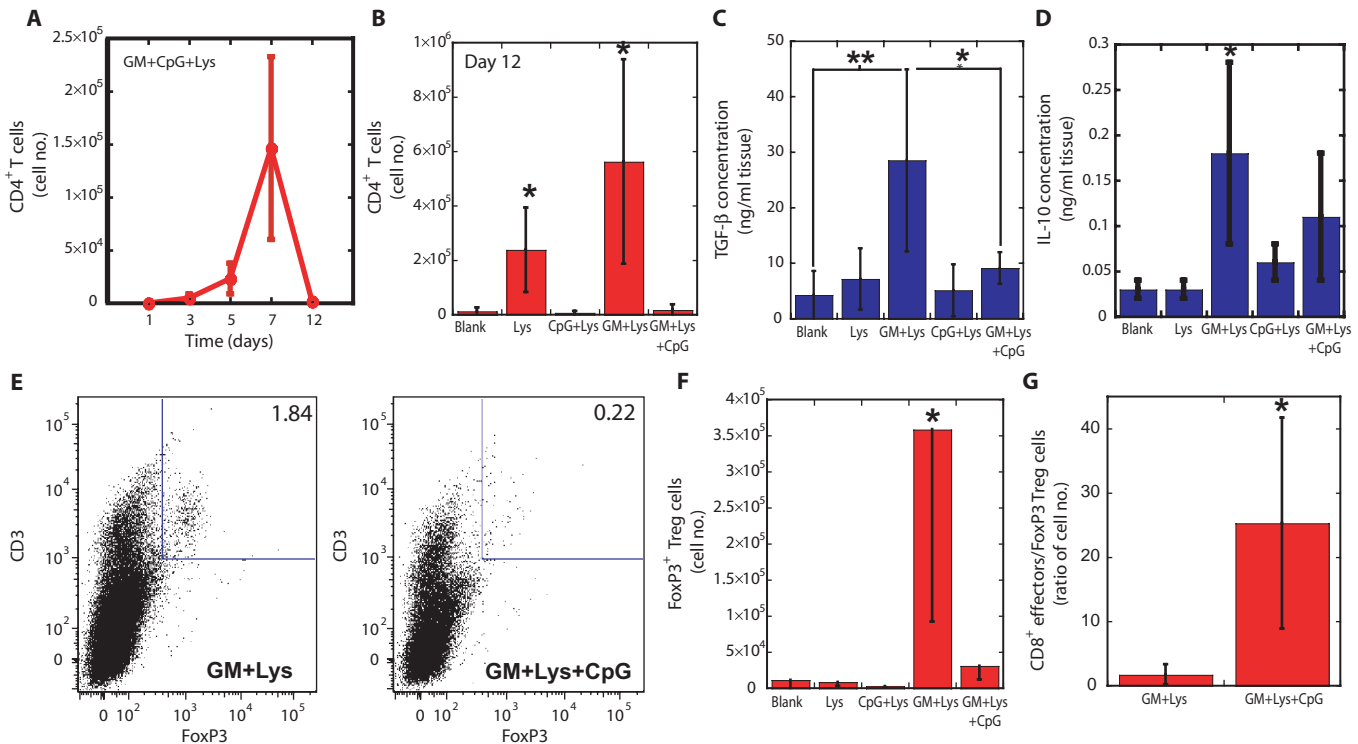


Fig. 6. Engineered PLG matrices attenuate FoxP3⁺ Treg cells and immunosuppressive cytokines. **(A)** Total number of CD3⁺CD4⁺ T cells isolated from PLG matrices loaded with GM-CSF, CpG-ODN, and tumor lysates as a function of time after implantation. **(B)** Number of CD4 T cells at day 12 after implantation in blank scaffolds (Blank) or in response to lysate alone (Lys) or in combination with CpG-ODN (CpG+Lys) or GM-CSF (GM+Lys) or both factors (GM+Lys+CpG). **(C and D)** The in vivo concentrations of TGF-β (C) and IL-10 (D) at day 12 after implantation at the implant site of blank scaffolds (Blank) or scaffolds presenting lysate alone (Lys) or in combination with CpG-ODN (CpG+Lys) or GM-CSF (GM+Lys) or both factors (GM+Lys+CpG). **(E)** FACS plots of cells isolated from explanted scaffolds and stained for the Treg cell markers CD3 and FoxP3. Cells were isolated

from PLG matrices incorporating GM-CSF and lysates (GM+Lys) or GM-CSF, lysates, and CpG-ODN (GM+Lys+CpG) at day 12 after implantation. Numbers in FACS plots indicate the percentage of the cell population positive for both markers. **(F)** Number of FoxP3⁺ Treg cells at day 12 after implantation in blank scaffolds (Blank) or in response to lysate alone (Lys) or in combination with CpG-ODN (CpG+Lys) or GM-CSF (GM+Lys) or both factors (GM+Lys+CpG). **(G)** Ratio of CD8a⁺ T cells versus FoxP3⁺ Treg cells residing within PLG scaffolds loaded with GM-CSF and lysates (GM+Lys) alone or in combination with CpG-ODN (GM+Lys+CpG) at day 12 after implantation. Values in (A), (B), (C), (D), (F), and (G) represent mean and SD (*n* = 4 or 5). **P* < 0.05, ***P* < 0.01 versus all other experimental conditions unless otherwise noted.

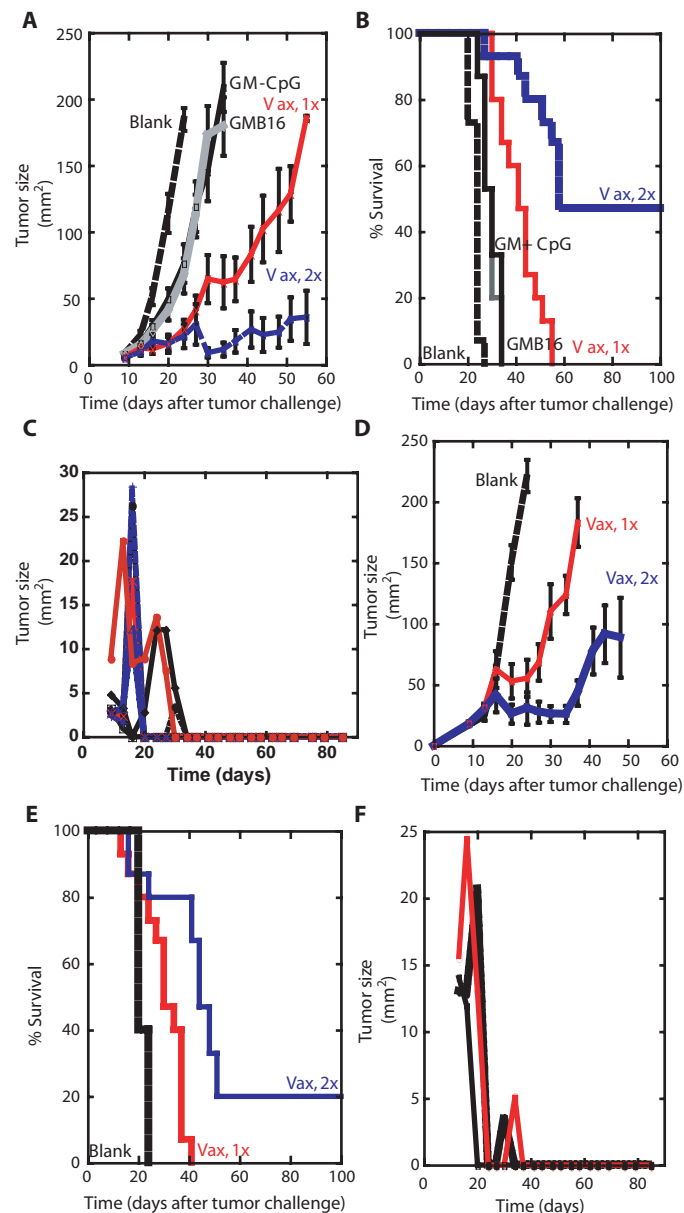


Fig. 7. Engineered PLG matrices stimulate the regression of established melanomas. (A and B) A comparison of the tumor growth (A) and survival (B) of mice bearing established melanoma tumors (inoculated with 5×10^5 B16-F10 cells and allowed to develop for 9 days) and treated with either blank PLG matrices (Blank) or matrices loaded with 3000 ng of GM-CSF and 100 μ g of CpG-ODN (GM-CpG). Mice were also treated once (Vax, 1x; at day 9) or twice (Vax, 2x; at days 9 and 19) with PLG matrices incorporating GM-CSF, CpG-ODN, and tumor lysates (Vax). Mice were also vaccinated with 5×10^5 irradiated, GM-CSF-transduced B16-F10 cells. (C) Individual tumor growth curves for each mouse surviving tumor challenge (5×10^5 cells) after a two-time treatment with PLG vaccines at days 9 and 19. (D and E) A comparison of the tumor growth (D) and survival (E) of mice bearing established melanoma tumors (inoculated with 5×10^5 B16-F10 cells and allowed to develop for 13 days) and treated with either blank PLG matrices (Blank) or once with PLG vaccines (Vax, 1x; at day 13) or twice (Vax, 2x; at days 13 and 23). (F) Individual tumor growth curves for each mouse surviving tumor challenge (5×10^5 cells) after a two-time treatment with PLG vaccines at days 13 and 23. Values in (A) and (D) [(A) to (F); $n = 15$ per condition] represent mean and SEM.

that generated about 1,200,000 pDCs and 600,000 CD8⁺ DCs (~43% of total DCs) in a total population of ~4.2 million DCs resulted in 90% survival in a subsequent tumor challenge. The engineered matrices appear to program T cell responses efficiently by providing a site of sustained immunostimulatory tumor antigen presentation, which evokes robust CTLs, both locally and systemically, and attenuates immune regulation mediated through TGF- β , IL-10, and FoxP3⁺ Treg cells. The kinetics of the adaptive immune response to our system suggest that CTLs manifested potent effector function, as vaccination resulted in a prototypical activation phase that gradually plateaued, followed by a contraction phase as antigen was cleared. Other vaccine formulations achieve only short-lived stimulation with infusions of protein or manipulated cells and may not trigger this T effector profile but instead induce at least partially dysfunctional T cells that are more likely to undergo exhaustion within the immunosuppressive tumor microenvironment (1–4).

Together, our results highlight a critical array of DC subtypes that are generated during the evolution of therapeutic antitumor responses in mice, which may provide a template for rational vaccine design more generally. Indeed, the vaccine system reported here might be adapted to modulate DC and CTL responses for the control of other solid cancers and perhaps chronic infections. Our approach might also facilitate the study of DC subset development and the mechanisms through which these subsets are coordinated in vivo for the eradication of established diseases. It is striking that tumor regression induced by these PLG vaccines outperformed gene-modified tumor cell vaccines in direct comparison and outperformed ex vivo DC vaccines reported in literature (1, 2, 4). This acellular biomaterial system was designed with components that either are FDA approved (PLG and GM-CSF) or have been used clinically (CpG-ODN) and do not require the maintenance and modification of live cell cultures. Together, these features suggest that this PLG system may have considerable advantages in terms of clinical application relative to other approaches reported to date. Scaling to humans will likely not require significant modification of the size or structure of the material but will require using effective human analogs (for example, human GM-CSF and CpG-ODN sequences) that evoke human DC and CTL responses. It is not clear whether the current combination of GM-CSF, CpG-ODN, and tumor antigen is the optimal formulation, and other dosing regimens or alternative TLR agonists or cytokines should be tested.

METHODS

Matrix fabrication

An 85:15, 120-kD copolymer of D,L-lactide and glycolide (PLG) (Alkermes) was used in a gas-foaming process to form porous PLG matrices (40). In brief, PLG microspheres encapsulating GM-CSF were first made with standard double emulsion (41). PLG microspheres were then mixed with 150 mg of the porogen, sucrose (sieved to a particle size between 250 and 425 μ m), and compression molded. The resulting disc was allowed to equilibrate within a high-pressure CO₂ environment, and a rapid reduction in pressure causes the polymer particles to expand and fuse into an interconnected structure (40). The sucrose was leached from the scaffolds by immersion in water, yielding scaffolds that were 90% porous. To incorporate tumor lysates into PLG scaffolds, we digested the biopsies of B16-F10 tumors that had grown subcutaneously in the backs of C57BL/6J mice (Jackson Laboratory) in collagenase (250 U/ml) (Worthington) and suspended at a

concentration equivalent to 10^7 cells per milliliter after filtration through 40- μ m cell strainers. The tumor cell suspension was subjected to four cycles of rapid freeze in liquid nitrogen and thaw (37°C) and then centrifuged at 400 rpm for 10 min. The supernatant (1 ml) containing tumor lysates was collected, incubated with the PLG microspheres, and lyophilized, and the resulting mixture was used in the high-pressure CO_2 process to foam macroporous PLG matrices incorporating tumor lysates. To incorporate CpG-ODNs into PLG scaffolds, we first condensed CpG-ODN 1826, 5'-tccatgacgttcctgacgtt-3' (Invivogen), with PEI ($M_n \sim 60,000$) molecules by dropping ODN 1826 solutions into PEI solution while vortexing the mixture (20, 42). The charge ratio between PEI and CpG-ODN ($\text{NH}_3^+:\text{PO}_4^-$) was kept constant at 7 during condensation. PEI-CpG-ODN condensate solutions were then vortexed with 60 μl of 50% (w/v) sucrose solution, lyophilized, and mixed with dry sucrose to a final weight of 150 mg. The sucrose containing PEI-CpG-ODN condensate was then mixed with blank, GM-CSF, and/or tumor lysate-loaded PLG microspheres to make PLG cancer vaccines.

In situ identification of DC subsets and T cells

Blank PLG matrices and matrices containing 3000 ng of GM-CSF alone or in combination with 1, 10, 50, or 100 μg of CpG-ODN (studies were also performed with tumor lysates copresented with either 3000 ng of GM-CSF or 100 μg of CpG-ODN alone or in combination) were implanted into subcutaneous pockets on the back of 7- to 9-week-old male C57BL/6J mice. For histological examination, scaffolds were excised and fixed in Z-fix solution (Anatech), embedded in paraffin, and stained with hematoxylin and eosin (H&E). To analyze DC recruitment, we excised scaffolds at various time points and digested the ingrown tissue into single-cell suspensions with a collagenase solution (250 U/ml; Worthington) that was agitated at 37°C for 45 min. The cell suspensions were then poured through a 40- μ m cell strainer to isolate cells from scaffold particles, and the cells were pelleted and washed with cold PBS and counted with a Z2 coulter counter (Beckman Coulter). To assess DC infiltration and activation, we stained subsets of the total cell population isolated from PLG matrices with primary antibodies (BD Pharmingen) conjugated to fluorescent markers to allow for analysis by flow cytometry. Allophycocyanin (APC)-conjugated CD11c (DC marker) and phycoerythrin (PE)-conjugated CD86 (B7, costimulatory molecule) stains were conducted for DC recruitment analysis, and APC-conjugated CD11c, fluorescein isothiocyanate (FITC)-conjugated CCR7, and PE-conjugated MHCII stains were conducted for DC programming analysis. To further delineate the presence of specific DC subsets, we stained cells with APC-conjugated CD11c and PE-conjugated PDCA-1 (pDC marker), APC-conjugated CD11c and PE-conjugated CD8 (CD8 DCs), or APC-conjugated CD11c and FITC-conjugated CD11b (CD11b DCs). To assess T cell infiltration, we performed PE-Cy7-conjugated CD3 stains in conjunction with APC-conjugated CD8a (CD8 T cells), FITC-conjugated CD4 (CD4 T cells), and PE-conjugated FoxP3 (Treg) and analyzed with flow cytometry. Cells were gated according to positive FITC, APC, and PE with isotype controls, and the percentage of cells staining positive for each surface antigen was recorded.

Tumor growth assays, protective cytokines, and TRP2 pentamer analysis

PLG scaffolds with melanoma tumor lysates and various dosages of GM-CSF and/or various quantities of PEI-CpG-ODN condensates were implanted subcutaneously into the lower left flank of C57BL/6J

mice. For prophylactic vaccinations, animals were challenged 14 days later with a subcutaneous injection of 10^5 B16-F10 melanoma cells [American Type Culture Collection (ATCC)] in the back of the neck. Animals were monitored for the onset of tumor growth ($\sim 1 \text{ mm}^3$) and killed for humane reasons when tumors grew to 20 to 25 mm (longest diameter).

To assess PLG vaccine efficacy in the therapeutic setting, we challenged C57BL/6J mice with a subcutaneous injection of 5×10^5 B16-F10 melanoma cells (ATCC) in the back of the neck. At either day 9 or day 13 after tumor challenge, PLG vaccines loaded with 3000 ng of GM-CSF, 100 μg of CpG-ODN, and tumor lysates were implanted subcutaneously into the lower left flank of C57BL/6J mice. A subset of mice was vaccinated again at 10 days after the initial vaccination (days 19 and 23).

To determine in vivo IL-12p70, IFN- α , IFN- γ , and TGF- β concentrations at the matrix implant site, we excised and digested the adjacent tissue with tissue protein extraction reagent (Pierce). After centrifugation, the concentrations of IL-12, IFN- α , IFN- γ , and TGF- β in the supernatant were then analyzed with enzyme-linked immunosorbent assay (R&D Systems) according to the manufacturer's instructions.

To determine the generation of TRP2-specific CTLs, we prepared single-cell suspensions from the spleens of mice immunized with PLG vaccines (lysate + 3000 ng of GM-CSF + 100 μg of CpG) at various time points. These cells were initially stained with APC-H-2Kb-TRP2 pentamers (Proimmune) and subsequently stained with PE-conjugated monoclonal antibody to CD8 (BD Pharmingen) before being analyzed by flow cytometry.

Statistical analysis

All values in the present study were expressed as mean \pm 1 SD unless otherwise noted.

The significant differences between the groups were analyzed by a Student's *t* test and a *P* value of <0.05 was considered significant.

SUPPLEMENTARY MATERIAL

www.sciencetranslationalmedicine.org/cgi/content/full/1/8/8ra19/DC1

Fig. S1. FACS plots of cells isolated from explanted scaffolds and stained for the DC marker CD11c and for activation markers MHCII and CCR7.

REFERENCES AND NOTES

1. S. A. Rosenberg, J. C. Yang, N. P. Restifo, Cancer immunotherapy: Moving beyond current vaccines. *Nat. Med.* **10**, 909–915 (2004).
2. C. A. Klebanoff, L. Gattinoni, N. P. Restifo, CD8 $^+$ T-cell memory in tumor immunology and immunotherapy. *Immunol. Rev.* **211**, 214–224 (2006).
3. R. M. Steinman, J. Banchereau, Taking dendritic cells into medicine. *Nature* **449**, 419–426 (2007).
4. E. Gilboa, DC-based cancer vaccines. *J. Clin. Invest.* **117**, 1195–1203 (2007).
5. G. Schuler, B. Schuler-Thurner, R. M. Steinman, The use of dendritic cells in cancer immunotherapy. *Curr. Opin. Immunol.* **15**, 138–147 (2003).
6. T. J. Curiel, D. T. Curiel, Tumor immunotherapy: Inching toward the finish line. *J. Clin. Invest.* **109**, 311–312 (2002).
7. S. H. Naik, P. Sathe, H. Y. Park, D. Metcalf, A. I. Proietto, A. Dakic, S. Carotta, M. O'Keeffe, M. Bahlo, A. Papenfuss, J. Y. Kwak, L. Wu, K. Shortman, Development of plasmacytoid and conventional dendritic cell subtypes from single precursor cells derived in vitro and in vivo. *Nat. Immunol.* **8**, 1217–1226 (2007).
8. A. O'Garra, G. Trinchieri, Are dendritic cells afraid of commitment? *Nat. Immunol.* **5**, 1206–1208 (2004).

9. A. D'Amico, L. Wu, The early progenitors of mouse dendritic cells and plasmacytoid dendritic cells are within the bone marrow hemopoietic precursors expressing Flt3. *J. Exp. Med.* **198**, 293–303 (2003).
10. A. M. Krieg, Development of TLR9 agonists for cancer therapy. *J. Clin. Invest.* **117**, 1184–1194 (2007).
11. T. Kawai, S. Akira, Innate immune recognition of viral infection. *Nat. Immunol.* **7**, 131–137 (2006).
12. J. J. O'Shea, R. Visconti, Type 1 IFNs and regulation of TH1 responses: Enigmas both resolved and emerge. *Nat. Immunol.* **1**, 17–19 (2000).
13. J. A. Villadangos, P. Schnorrer, Intrinsic and cooperative antigen-presenting functions of dendritic-cell subsets in vivo. *Nat. Rev. Immunol.* **7**, 543–555 (2007).
14. P. Schnorrer, G. M. Behrens, N. S. Wilson, J. L. Pooley, C. M. Smith, D. El-Sukkari, G. Davey, F. Kupresanin, M. Li, E. Maraskovsky, G. T. Belz, F. R. Carbone, K. Shortman, W. R. Heath, J. A. Villadangos, The dominant role of CD8⁺ dendritic cells in cross-presentation is not dictated by antigen capture. *Proc. Natl. Acad. Sci. U.S.A.* **103**, 10729–10734 (2006).
15. K. Shortman, S. H. Naik, Steady-state and inflammatory dendritic-cell development. *Nat. Rev. Immunol.* **7**, 19–30 (2007).
16. J. A. Hamilton, GM-CSF in inflammation and autoimmunity. *Trends Immunol.* **23**, 403–408 (2002).
17. M. C. Dieu, B. Vanbervliet, A. Vicari, J. M. Bridon, E. Oldham, S. Ait-Yahia, F. Brière, A. Zlotnik, S. Lebecqque, C. Caux, Selective recruitment of immature and mature dendritic cells by distinct chemokines expressed in different anatomic sites. *J. Exp. Med.* **188**, 373–386 (1988).
18. G. Dranoff, E. Jaffee, A. Lazenby, P. Golumbek, H. Levitsky, K. Brose, V. Jackson, H. Hamada, D. Pardoll, R. C. Mulligan, Vaccination with irradiated tumor cells engineered to secrete murine granulocyte-macrophage colony-stimulating factor stimulates potent, specific, and long-lasting anti-tumor immunity. *Proc. Natl. Acad. Sci. U.S.A.* **90**, 3539–3543 (1993).
19. B. Pulendran, J. Banchereau, S. Burkeholder, E. Kraus, E. Guinet, C. Chalouni, D. Caron, C. Maliszewski, J. Davoust, J. Fay, K. Palucka, Flt3-ligand and granulocyte colony-stimulating factor mobilize distinct human dendritic cell subsets in vivo. *J. Immunol.* **165**, 566–572 (2000).
20. O. A. Ali, N. Huebsch, L. Cao, G. Dranoff, D. J. Mooney, Infection-mimicking materials to program dendritic cells in situ. *Nat. Mater.* **8**, 151–158 (2009).
21. N. Mach, S. Gillessen, S. B. Wilson, C. Sheehan, M. Mihm, G. Dranoff, Differences in dendritic cells stimulated in vivo by tumors engineered to secrete granulocyte-macrophage colony-stimulating factor or Flt3-ligand. *Cancer Res.* **60**, 3239–3246 (2000).
22. E. Daro, B. Pulendran, K. Brasel, M. Teepe, D. Pettit, D. H. Lynch, D. Vremec, L. Robb, K. Shortman, H. J. McKenna, C. R. Maliszewski, E. Maraskovsky, Polyethylene glycol-modified GM-CSF expands CD11b^{high}CD11c^{high} but not CD11b^{low}CD11c^{high} murine dendritic cells in vivo: A comparative analysis with Flt3 ligand. *J. Immunol.* **165**, 49–58 (2000).
23. C. Fonseca, G. Dranoff, Capitalizing on the immunogenicity of dying tumor cells. *Clin. Cancer Res.* **14**, 1603–1608 (2008).
24. J. D. Farrar, H. Asnagli, K. M. Murphy, T helper subset development: Roles of instruction, selection, and transcription. *J. Clin. Invest.* **109**, 431–435 (2002).
25. D. Skokos, M. C. Nussenzweig, CD8⁺ DCs induce IL-12-independent Th1 differentiation through Delta 4 Notch-like ligand in response to bacterial LPS. *J. Exp. Med.* **204**, 1525–1531 (2007).
26. J. M. den Haan, S. M. Lehar, M. J. Bevan, CD8⁺ but not CD8[−] dendritic cells cross-prime cytotoxic T cells in vivo. *J. Exp. Med.* **192**, 1685–1696 (2000).
27. M. Moser, K. M. Murphy, Dendritic cell regulation of TH1-TH2 development. *Nat. Immunol.* **1**, 199–205 (2000).
28. D. Jankovic, M. C. Kullberg, S. Hieny, P. Caspar, C. M. Collazo, A. Sher, In the absence of IL-12, CD4⁺ T cell responses to intracellular pathogens fail to default to a Th2 pattern and are host protective in an IL-10^{−/−} setting. *Immunity* **16**, 429–439 (2002).
29. V. E. Schijns, B. L. Haagmans, C. M. Wierda, B. Kruithof, I. A. Heijnen, G. Alber, M. C. Horzinek, Mice lacking IL-12 develop polarized Th1 cells during viral infection. *J. Immunol.* **160**, 3958–3964 (1998).
30. J. Magram, J. Sfarra, S. Connaughton, D. Faherty, R. Warrier, D. Carvajal, C. Y. Wu, C. Stewart, U. Sarmiento, M. K. Gately, IL-12-deficient mice are defective but not devoid of type 1 cytokine responses. *Ann. N.Y. Acad. Sci.* **795**, 60–70 (1996).
31. W. W. Overwijk, M. R. Theoret, S. E. Finkelstein, D. R. Surman, L. A. de Jong, F. A. Vyth-Dreese, T. A. Delleman, P. A. Antony, P. J. Spiess, D. C. Palmer, D. M. Heimann, C. A. Klebanoff, Z. Yu, L. N. Hwang, L. Feigenbaum, A. M. Kruisbeek, S. A. Rosenberg, N. P. Restifo, Tumor regression and autoimmunity after reversal of a functionally tolerant state of self-reactive CD8⁺ T cells. *J. Exp. Med.* **198**, 569–580 (2003).
32. Y. Tamura, P. Peng, K. Liu, M. Daou, P. K. Srivastava, Immunotherapy of tumors with autologous tumor-derived heat shock protein preparations. *Science* **278**, 117–120 (1997).
33. S. A. Quezada, K. S. Peggs, M. A. Curran, J. P. Allison, CTLA4 blockade and GM-CSF combination immunotherapy alters the intratumor balance of effector and regulatory T cells. *J. Clin. Invest.* **116**, 1935–1945 (2006).
34. M. Jinushi, Y. Nakazaki, M. Dougan, D. R. Carrasco, M. Mihm, G. Dranoff, MFG-E8-mediated uptake of apoptotic cells by APCs links the pro- and antiinflammatory activities of GM-CSF. *J. Clin. Invest.* **117**, 1902–1913 (2007).
35. F. S. Hodi, M. Butler, D. A. Oble, M. V. Seiden, F. G. Haluska, A. Kruse, S. Macrae, M. Nelson, C. Canning, I. Lowy, A. Korman, D. Lutz, S. Russell, M. T. Jaklitsch, N. Ramaia, T. C. Chen, D. Neuberger, J. P. Allison, M. C. Mihm, G. Dranoff, Immunologic and clinical effects of antibody blockade of cytotoxic T lymphocyte-associated antigen 4 in previously vaccinated cancer patients. *Proc. Natl. Acad. Sci. U.S.A.* **105**, 3005–3010 (2008).
36. M. Jinushi, F. S. Hodi, G. Dranoff, Enhancing the clinical activity of granulocyte-macrophage colony-stimulating factor-secreting tumor cell vaccines. *Immunol. Rev.* **222**, 287–298 (2008).
37. M. E. Dudley, J. R. Wunderlich, J. C. Yang, R. M. Sherry, S. L. Topalian, N. P. Restifo, R. E. Royal, U. Kammula, D. E. White, S. A. Mavroukakis, L. J. Rogers, G. J. Gracia, S. A. Jones, D. P. Manganelli, M. M. Pelletier, J. Gea-Banacloche, M. R. Robinson, D. M. Berman, A. C. Filie, A. Abati, S. A. Rosenberg, Adoptive cell transfer therapy following non-myeloablative but lymphodepleting chemotherapy for the treatment of patients with refractory metastatic melanoma. *J. Clin. Oncol.* **23**, 2346–2357 (2005).
38. H. Kanzler, F. J. Barrat, E. M. Hessel, R. L. Coffman, Therapeutic targeting of innate immunity with Toll-like receptor agonists and antagonists. *Nat. Med.* **13**, 552–559 (2007).
39. P. Serafini, R. Carbley, K. A. Noonan, G. Tan, V. Bronte, I. Borrello, High-dose granulocyte-macrophage colony-stimulating factor-producing vaccines impair the immune response through the recruitment of myeloid suppressor cells. *Cancer Res.* **64**, 6337–6343 (2004).
40. L. D. Harris, B. S. Kim, D. J. Mooney, Open pore biodegradable matrices formed with gas foaming. *J. Biomed. Mater. Res.* **42**, 396–402 (1998).
41. S. Cohen, T. Yoshioka, M. Lucarelli, L. H. Hwang, R. Langer, Controlled delivery systems for proteins based on poly(lactic/glycolic acid) microspheres. *Pharm. Res.* **8**, 713–720 (1991).
42. Y. C. Huang, M. Connell, Y. Park, D. J. Mooney, K. G. Rice, Fabrication and in vitro testing of polymeric delivery system for condensed DNA. *J. Biomed. Mater. Res. A* **67**, 1384–1392 (2003).
43. Acknowledgments: We thank Jebecka Hudak for assistance with cell culturing and Brian Tilton and Patricia Rogers for assistance with flow cytometry.
Funding: NIH–National Institute of Dental and Craniofacial Research grant R01-DE019917; Department of Defense (BC084682 Idea Award); Harvard Catalyst, the Harvard Clinical and Translational Science Center (NIH grant 1 UL1 RR 025758-01); financial contributions from participating institutions; and InCytu Inc.
Author contributions: The experiments were designed by O.A.A., D.E., D.J.M., and G.D. and carried out by O.A.A. and D.E. The manuscript was written by O.A.A., D.E., G.D., and D.J.M. The principal investigator is D.J.M.
Competing interests: O.A.A. and D.E. are now working for InCytu Inc. to commercialize the technology described in this paper and have stock options with the company. D.J.M. is on the Board of Directors of, and owns stock options with, InCytu Inc. O.A.A., G.D., and D.J.M. have filed an application for a patent on the technology described in this manuscript.

Submitted 31 August 2009
 Accepted 5 November 2009
 Published 25 November 2009
 10.1126/scitranslmed.3000359

Citation: O. A. Ali, D. Emerich, G. Dranoff, D. J. Mooney, In situ regulation of DC subsets and T cells mediates tumor regression in mice. *Sci. Transl. Med.* **1**, 8ra19 (2009).